MACROPORE NETWORKS AFFECT THE FILTERING FUNCTION OF SOILS

Karin Müller[1], Markus Deurer[2], Malcolm McLeod[3], Iain Young[4], John Scott[5] and Brent E Clothier[2]

[1]The NZ Institute for Plant & Food Research (PFR), Systems Modelling, Hamilton
Email: karin.mueller@plantandfood.co.nz
[2]PFR, Systems Modelling, Palmerston North
[3]Landcare Research, Hamilton
[4]University of New England, Armidale, Australia
[5]Landcare Research, Christchurch

Soils deliver the ecosystem service of filtering. But filtering capacities differ among soils such that the quick transport of agrichemicals into aquifers cannot be excluded. We hypothesized that a soil's filtering capacity depends on its macropore structure, which is linked to soil texture. Tension disc infiltrometry can be used to measure hydraulic properties near saturation. The differentiation between hydrologically active and non-active pores at a given tension is an indirect method to characterize macropore continuity. Water flow through macropores is a function of the macropore size distribution, tortuosity and the connectivity of macropores. These characteristics can be directly derived by 3D X-ray computer tomography (CT). Our objective was to analyze the macropore network and to characterize the resulting filtering performance of soils with contrasting structures. For this purpose, two soils under pasture with known filtering behaviour for microbes were selected. The soils were an Allophanic Soil (excellent filter) and a Gley Soil (poor filter). Each soil was separated into three horizons assuming that each horizon had a specific macropore structure. In March 2011, infiltration near saturation was measured in the field; hydraulic conductivity K_0 and flow-weighted mean macropore diameter α for each soil horizon were derived. We extracted intact soil cores from the centre of the infiltration areas and determined the macropore architecture by X-ray CT. The results were validated with bromide leaching experiments through intact soil cores. Dye tracer experiments visualized flow patterns in situ. Our results confirmed the better filtering capacity of the Allophanic Soil. The soil's comparatively low macroporosity was coupled with a high connectivity of the smaller macropores which led to a more homogeneous matrix flux. Similarly, all measurements confirmed the poorer filtering capacity of the Gley Soil, which had a bi-modal pore system with a few very large, but well connected macropores. This resulted in preferential flows. We identified the macroporosity, mean pore diameter and connectivity as the relevant 'form' parameters to describe the 'function' of solute filtering.

Introduction

The importance of macropores as preferential pathways of water, air, and chemicals in the soil has been widely recognized (Clothier et al., 2008). Water flux through macropores can be as high as 70% of the total flux and thus a governing process for water and solute transport in soils (Watson and Luxmoore, 1986). We adopted Jarvis's (2007) definition of macropores as pores with a diameter larger than 0.3 mm and assumed that these pores are responsible for

macropore (= preferential) flow and poor filtering of soils. Macropores form a complex connected network made of earthworm channels, fissures, roots and inter-aggregate voids. Our hypothesis was that a soil's filtering capacity depends on its macropore network, which is closely linked to soil texture. Often, soils with high clay contents are strongly structured and exhibit more macropore flow than soils with lower clay contents. The structure of macropore networks can be directly investigated with non-invasive techniques, such as 3D X-ray Computed Tomography (CT). To bridge the gap between soil structure and function, relevant soil macropore features need to be identified and quantified. Our objectives were (1) to measure the filtering capacities of soils with different textures, (2) to reconstruct the macropore network of these soils, and (3) to investigate the role of macropore topological features on the macroscopic flow and transport characteristics derived from *in situ* infiltration measurements and solute transport experiments.

Methods

Two soils under permanent pasture were selected representing contrasting structure, which were known to differ in their filtering behaviour for microbes (Pang et al., 2008). The soils were an Allophanic Soil (Waihou Gritty Silt Loam (McLeod, 1992); excellent filter) and a Gley Soil (Netherton Clayey Gley Loam (McLeod et al., 2001); poor filter). All experiments were conducted in three depths, chosen to represent three distinct soil genetic horizons: the topsoil (Ah), the upper (Bw1 or Bg1) and lower subsoil (Bw2 or Bg2) layers of the two soils.

In March 2011, we measured infiltration rates at four different tensions (h = -10, -20, -40, -70 mm) in triplicate. We derived the unsaturated hydraulic conductivity K_0 at several tensions following Reynolds and Elrick (2005). According to the capillary rise equation, infiltration at tensions of -10, -20, -40 and -70 mm will exclude pores from flow processes, which have equivalent pore radii greater than 1.48, 0.74, 0.37 and 0.21 mm, respectively. We used the infiltrometer results at steady state at a given tension to estimate the mean pore size weighted by flow α, at this tension (Reynolds and Elrick, 1991). A large α indicates that the unsaturated flow is dominated by gravitational force, meaning that macropore flow dominates over matrix flow. We extracted intact soil cores from the centre of the infiltration areas and determined the macropore architecture of the soils by X-ray Computed Tomography (CT). We applied the image analysis protocols developed by Deurer et al. (2009). A dye tracer experiment with Brilliant Blue FCF visually discerned the flow pathways in the three horizons of the two soils. In May 2013, we extracted intact soil cores (100 mm diameter, 75 mm length) from each of the six soil horizons. An approximately 25-mL pulse of bromide was exogenously applied to the cores with a tension disc infiltrometer set to -15 mm. We leached the bromide through the cores under the same conditions. The outflow rates and bromide concentrations of the leachate samples were determined. To quantify the transport dynamics in the soil cores, we used the breakthrough curves (BTCs) of the relative concentrations, being the concentration C in outflow sample i divided by the concentration in the incident solute pulse, C_i/C_0, as a function of the pore volume. The transport experiments were modelled using the convection-dispersion equation (CDE) for homogeneous flow or the two-region non-equilibrium model. Model parameters were obtained by fitting the models to the measured BTCs, using the CXTFIT curve-fitting program in inverse mode (Toride et al., 1995).

A general analysis of variance with two fixed effects (soil type, horizon) was used to determine if the macropore properties of the Gley Soil and the Allophanic Soil were significantly different. We interpreted the differences between macropore properties to be

significant if they were larger than their respective least significant differences (LSD) at the 95% confidence level ($P \leq 0.05$). Stepwise regression analysis was used to correlate the macropore characteristics derived from X-ray CT to the near-saturated hydraulic conductivity based on tension infiltrometry measurements and dispersivity based on the bromide transport experiments.

Results and discussion

1. Measuring and modelling water flow and transport of bromide

The peak concentrations of all bromide BTCs arrived earlier than one pore volume with the exception of those for the two subsoils of the Allophanic Soil (Fig. 1). The early breakthrough of bromide coupled with tailing implies that water flow was not in equilibrium and that macropore flow took place. The steep front of the BTCs reflects that bromide was transported through macropores, and the tailing indicates that exchange processes with the matrix took place. In contrast to this preferential movement, bromide was slightly retarded in the Allophanic subsoils (Fig. 1), which can be explained by the positive charge of allophones at the soil's pH (Pang et al., 2008). In these two horizons, bromide concentrations peaked at or just after one pore volume, and the BTCs were relatively symmetrical (Fig. 1). Only the measured BTCs of the Bw2-horizon of the Allophanic Soil were well described with the CDE with R^2>0.92. The average dispersivity was 2.1 cm.

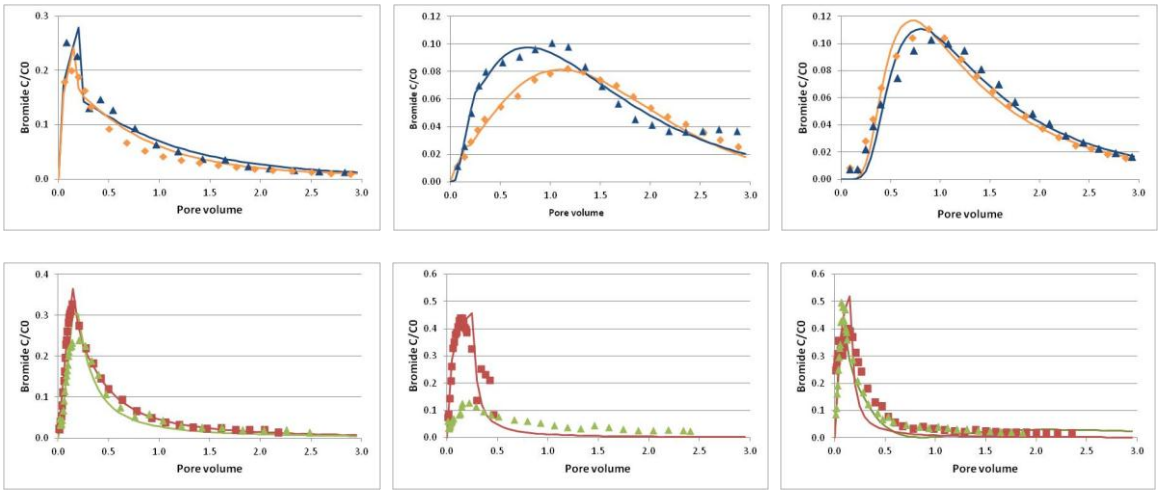

Figure 1. *Measured (symbols) and modelled (lines) bromide breakthrough curves in the topsoils (left) and the subsoils (Bw1, Bg1; middle and Bw2, Bg2; right) of the Allophanic Soil (top) and the Gley Soil (bottom). In the Allophanic subsoil, the measured data fit the Convection-Dispersion-Equation with R^2-values >0.9. In all other soils, the two-regional non-equilibrium model was used, R^2-values >0.8. The experiments were conducted in duplicate.*

All other measured bromide BTCs were reasonably described with the two-region mobile-immobile model. The mobile-immobile model requires parameters that cannot be measured. They were derived through inverse fitting. The dependence on such inverse modelling procedures to derive parameters including the dispersivity, the mass transfer coefficient and the fraction of mobile water, which are needed to predict the filtering capacity of structured soils, severely limits our predictive capability. Vervoort et al. (1999) suggested that a conservative critical value for the occurrence of preferential flow might be dispersivity values

greater than the length of the soil core. In our experiments, this threshold was only exceeded for the experiments with the Gley Soil. In contrast, in the topsoil and Bw1-horizon of the Allophanic Soil, the dispersivity ranged between 0.003 and 7.5 cm. These results were confirmed by our dye experiments. The downward movement of dye was relatively homogeneous in all horizons of the Allophanic Soil, and preferential in all Gley Soil horizons.

2. Deriving soil hydraulic parameters

The unsaturated hydraulic conductivity K_0 was significantly (P<0.05) higher in the Allophanic than in the Gley Soil at all tensions and decreased significantly (P<0.05) with depth in both soils (Fig. 2). However, in all bromide transport experiments conducted at -15 mm, the bromide concentrations peaked earlier in the Gley than the Allophanic Soils. This suggests the importance of macropores in the Gley Soil.

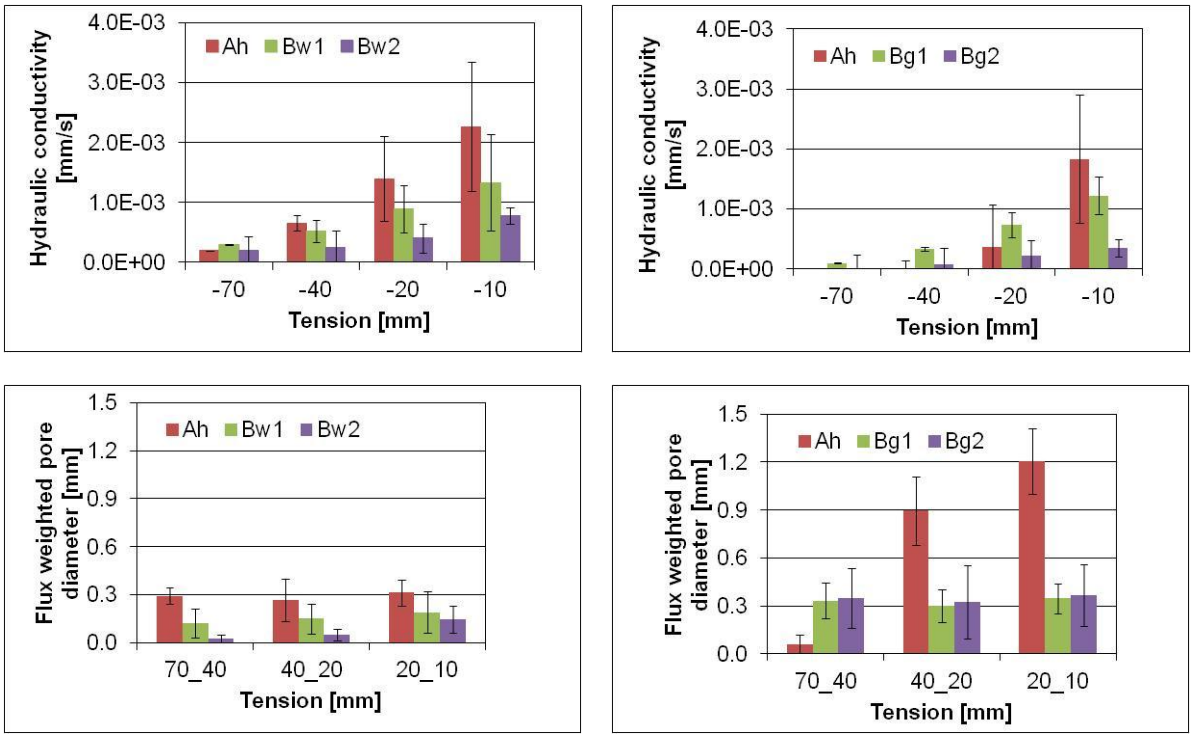

Figure 2. *Hydraulic conductivities near saturation (top) and flow-weighted mean macropore diameters (bottom) of the Allophanic Soil (left) and the Gley Soil (right) for three soil horizons (Ah - topsoil, Bw1, Bg1 - upper subsoil, Bw2, Bg2 - lower subsoil). The bars denote the standard deviation of three replicates.*

Capillary tension can be related to an equivalent pore diameter and thus, the tension applied with an infiltrometer can be used to estimate the range of pores contributing to the measured infiltration. The flux-weighted mean macropore diameter α defines mean characteristic pore sizes that are hydraulically functioning at a specific tension. Consistent with the bromide transport experiments, the flux-weighted mean macropore diameter at the two tension pairs closest to saturation was significantly (P<0.05) higher in the Gley Soil than in the Allophanic Soil (Fig. 2). For all tensions, α was below 0.3 mm, the threshold for macropores according to Jarvis (2007), for the Allophanic Soil. For the Gley Soil, α was below 0.3 mm only in the subsoil at all tensions. In the topsoil, at least at tensions smaller than -40 mm water, α was significantly (P<0.05) greater than 0.3 mm. The largest flux-weighted mean macropore

diameter α of 1.2 mm was found for the tension pair closest to saturated conditions in the Gley topsoil. However, these large pores/cracks in the Gley Soil must be rather infrequent because the related unsaturated hydraulic conductivity was lower than that of the Allophanic Soil at the same tension. In contrast, the Allophanic Soil must have many well connected narrower macropores to have a larger unsaturated hydraulic conductivity than the Gley Soil in spite of a smaller flux-weighted mean macropore diameter.

3. Reconstructing macropore networks based on X-ray CT-images

The CT measurements verified the above assumptions on macropore size and density for the two soils. Figure 3 shows a visualisation of the reconstructed macropore networks of the subsoils of the Gley and Allophanic Soils. The mean macropore radius of the Gley Soil was significantly (P<0.05) greater than that of the Allophanic Soil. Its decrease with depth was not significant for either soil. The pore size distribution in the Allophanic Soil was characterized by a larger number of smaller macropores connected to the larger macropores, and a lack of extreme large macropores (Fig. 4). Generally, the macropores in the Allophanic Soil had a higher coordination number. The Gley Soil's macropore size distribution was distinctively different with its clay peds clearly defined by larger macropores. In addition, the CT-measurements identified a significantly (P<0.05) greater macroporosity for the Gley Soil than for the Allophanic Soil. The macroporosity of the topsoils was significantly (P<0.05) greater than that of the subsoils in both soils. While macroporosity can be measured with simpler techniques, the CT images provide additional information on the architecture of the macropore network, such as the number of pores of specific diameters, coordination number and connectivity of pores.

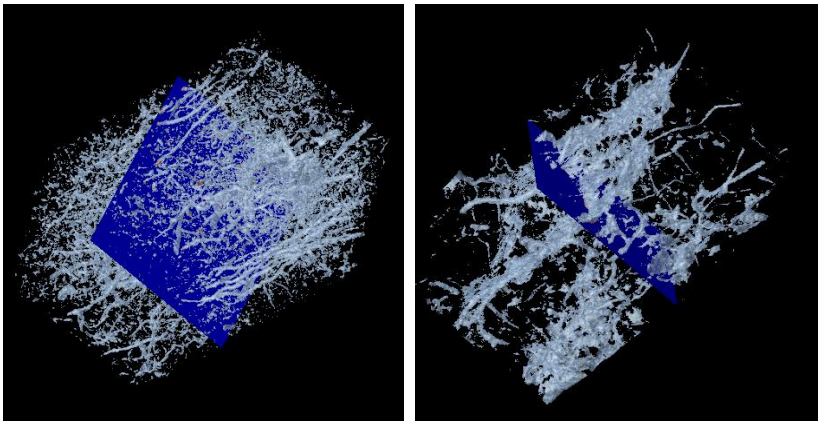

Figure 3. *Visualization of the typical macropore network of the lower subsoil of the Allophanic Soil (left) and the Gley Soil (right) derived with 3D X-ray Computer Tomography.*

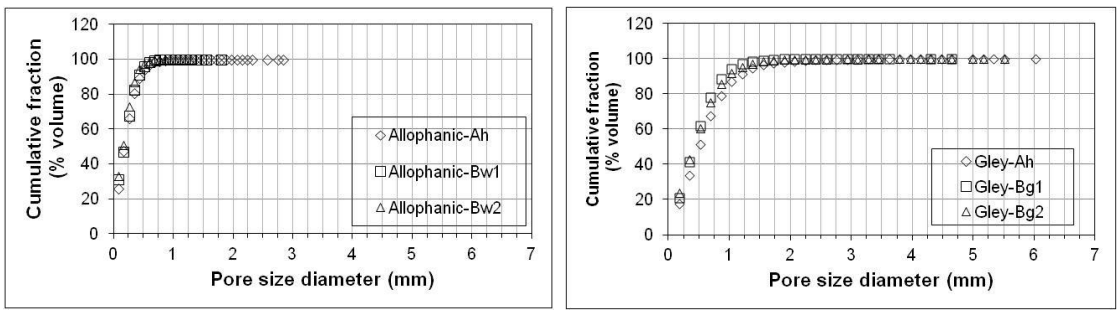

Figure 4. The *macropore diameter size distribution of the Allophanic Soil (left) and the Gley Soil (right).*

4. Role of macropore topological features on macroscopic flow and transport

The differences in macropore characteristics of the two soil types and in the three horizons imply that the soil functional properties would be different between the two soil types and would also change with depth in the two soils. Based on our image analysis, we expect that macropore flow would be more important in the Gley Soil than in the Allophanic Soil, and that its importance would cease with depth. This is exactly what we found in our transport experiments. The results of the CT-images highlight that more macropores with higher coordination numbers lead to a better lateral mixing and filtering of contaminants. The total macroporosity of the Gley Soil was significantly higher than that of the Allophanic Soil, while the connectivity of the macropore systems of both soils was comparable. Macropore size distribution was the key factor explaining the different filtering capacity of these two soils: The Gley Soil has a significantly larger mean pore diameter driven by a few, extremely large macropores, reflecting the structure of the clay loam soil and its tendency to form inter-pedal cracks, which, even if their number was relatively small, enhanced preferential flow during near-saturated conditions.

A correlation analysis showed that macroporosity, mean macropore radius and connectivity were highly correlated. In a multiple regression, 69% of the variability in the logarithm of the unsaturated hydraulic conductivity estimated at a tension of -10 mm was explained in all horizons of both soils with the logarithm of the macroporosity, the logarithm of the average pore diameter and the Euler number as significant variables. Dispersivity, as derived through inverse fitting using the two-regional non-equilibrium model for the Gley Soil was significantly and negatively correlated with macroporosity. For the Allophanic soil, dispersivity was positively and significantly correlated with the mean macropore radius. These results indicate that macropore characteristics useful for predicting unsaturated water flow and solute transport through undisturbed soils include macroporosity, connectivity and the mean pore diameter.

Conclusions

Our measurement dualism discerned flow mechanisms. The better filtering capacity of the Allophanic Soil was confirmed as the comparatively low macroporosity was coupled with a high connectivity of the smaller macropores which led to a more homogeneous matrix flux. Similarly, all measurements confirmed the poorer filtering capacity of the Gley Soil, which had a bi-modal pore system with a few very large, but well connected macropores. This resulted in preferential flows. We identified the macroporosity, mean pore diameter and connectivity as relevant ‘form’ parameters to describe the ‘function’ of flow and transport.

The results from this study provide improved quantitative evaluation of soil macropore features that have significant implications for non-equilibrium flow prediction. Linking macropore characteristics to soil functional properties, such as, for example, the unsaturated hydraulic conductivity and dispersivity in this study will help to better understand and model flow processes. This can lead to management practices which maintain and enhance soil functions.

Acknowledgements

This research was funded through Landcare Research and the Ministry for Business, Innovation and Employment (Contract 1314-32-001K).

References

Clothier, B.E., Green, S.R., Deurer, M., 2008. Preferential flow and transport in soil: progress and prognosis. European Journal of Soil Science 59(1), 2-13.

Deurer, M., Grinev, D., Young, I., Clothier, B.E., Müller, K., 2009. The impact of soil carbon management on soil macropore structure: a comparison of two apple orchard systems in New Zealand. European Journal of Soil Science 60, 945-955.

Jarvis, N., Larsbo, M., Roulier, S., Lindahl, A., Persson, L., 2007. The role of soil properties in regulating non-eqilibrium macropore flow and solute transport in agricultural topsoils. European Journal of Soil Science 58, 282-292.

Jarvis, N.J., 2007. A review of non-equilibrium water flow and solute transport in soil macropores: principles, controlling factors and consequences for water quality. European Journal of Soil Science 58(3), 523-546.

McLeod, D.J., 1992. Soils of part northern Matamata country, North Island, New Zealand, DSIR Land Resources, Hamilton, New Zealand.

McLeod, M., Aislabie, J., Smith, J., Fraser, R., Roberts, A., Taylor, M., 2001. Viral and chemical tracer movement through contrasting soils. J. Environ. Qual. 30, 2134-2140.

Pang, L., McLeod, M., Aislabie, J., Simunek, J., Close, M., Hector, R., 2008. Modeling transport of microbes in ten undisturbed soils under effluent irrigation. Vadose Zone J 7(1), 97-111.

Reynolds, W.D., Elrick, D.E., 1991. Determination of hydraulic conductivity using a tension infiltrometer. Soil Sci. Soc. Am. J. 55, 633-639.

Reynolds, W.D., Elrick, D.E., 2005. Measurement and Characterization of Soil Hydraulic Processes. In: J. Álvarez-Benedí, R. Munoz-Carpena (Eds.), Soil-Water-Solute Process Characterization. CRC Press, Boca Raton, pp. 197-252.

Toride, N., Leij, F.J., van Genuchten, M.T., 1995. The CXTFIT code for estimating transport parameters from laboratory or field tracer experiments. Research Report 137, U.S. Salinity Laboratory Agricultural Research Service, U. S. Department of Agriculture, Riverside, California.

Vervoort, R.W., Radcliffe, D.E., West, L.T., 1999. Soil structure development and preferential solute flow. . Wat. Resourc. Res. 35(4), 913-928.

Watson, K.W., Luxmoore, R.J., 1986. Estimating Macroporosity in a Forest Watershed by use of a Tension Infiltrometer. Soil Sci. Soc. Am. J. 50(3), 578-582.